Three-dimensional multi Bioluminescent Sources Reconstruction based on Adaptive Finite Element Method

Xibo Ma[1], Jie Tian[1*], Bo Zhang[2], Xing Zhang[1],Zhenwen Xue[1], Di Dong[1], Dong Han[1]
1 Medical Image Processing Group, Institute of Automation, Chinese Academy of Sciences, P. O. Box 2728, Beijing 100190, China
2 Sino-Dutch Biomedical and Information Engineering School of Northeastern University, Shenyang 110819, China

ABSTRACT

Among many optical molecular imaging modalities, bioluminescence imaging (BLI) has more and more wide application in tumor detection and evaluation of pharmacodynamics, toxicity, pharmacokinetics because of its noninvasive molecular and cellular level detection ability, high sensitivity and low cost in comparison with other imaging technologies. However, BLI can not present the accurate location and intensity of the inner bioluminescence sources such as in the bone, liver or lung etc. Bioluminescent tomography (BLT) shows its advantage in determining the bioluminescence source distribution inside a small animal or phantom. Considering the deficiency of two-dimensional imaging modality, we developed three-dimensional tomography to reconstruct the information of the bioluminescence source distribution in transgenic mOC-Luc mice bone with the boundary measured data. In this paper, to study the osteocalcin (OC) accumulation in transgenic mOC-Luc mice bone, a BLT reconstruction method based on multilevel adaptive finite element (FEM) algorithm was used for localizing and quantifying multi bioluminescence sources. Optical and anatomical information of the tissues are incorporated as *a priori* knowledge in this method, which can reduce the ill-posedness of BLT. The data was acquired by the dual modality BLT and Micro CT prototype system that was developed by us. Through temperature control and absolute intensity calibration, a relative accurate intensity can be calculated. The location of the OC accumulation was reconstructed, which was coherent with the principle of bone differentiation. This result also was testified by *ex vivo* experiment in the black 96-plate well using the BLI system and the chemiluminescence apparatus.

Keywords*:* bioluminescent tomography (BLT), finite element method (FEM), transgenic mice, reconstruction

1. INTRODUCTION

Molecular imaging including bioluminescent imaging and fluorescent imaging can help to study the biological process in cellular and molecular level with its high-sensitivity characteristics.[1-3] Bioluminescent imaging can noninvasively discern the light-emitting cells from the general cells.

In recent years, bioluminescent imaging (BLI) has been widely used in biological and drug development.[4-6] BLI can only present the two-dimensional information of imaging target, so Bioluminescence tomography methods have been more and more deeply studied in the molecular imaging. Many algorithms have been proposed for reconstructing the light source distribution, such as Tikhonov regularization based on adaptive finite elements,[7] a temperature-modulated bioluminescence tomography method,[8] a born-type approximation bioluminescence tomography method,[9] etc. Although many algorithms had been studied in the phantom experiments and simulation experiments, little methods had been applied in the actual biological and drug research.

Osteocalcin (OC) is a bone tissue-specific protein expressed by osteoblasts, odontoblasts, and

Medical Imaging 2011: Biomedical Applications in Molecular, Structural, and Functional Imaging, edited by John B. Weaver, Robert C. Molthen, Proc. of SPIE Vol. 7965, 79650B · © 2011 SPIE · CCC code: 0277-786X/11/$18 · doi: 10.1117/12.878049

hypertrophic chondrocytes at the onset of tissue mineralization and it accumulates in the bone extracellular matrix. Many research institutions carried out extensive studies about osteocalcin. The corresponding results have been published. However, there was not a three-dimensional imaging study on the osteocalcin concentration. Here, we applied the multilevel adaptive finite element algorithm to determine multi-bioluminescence sources distribution in transgenic mOC-Luc mice accurately, and evaluate the efficacy and merits of the *in vivo* method by comparing the traditional *ex vivo* biology method.

2. METHOD AND EXPERIMENT

2.1 Transgenic mouse model

The transgenic mOC-Luc (mouse osteocalcin promoter-luciferase construct) mice were obtained by microinjection, which harbored a luciferase marker gene under the regulation of the mouse osteocalcin (mOC) promoter. Osteocalcin (OC) is a bone tissue-specific protein expressed by osteoblasts, odontoblasts, and hypertrophic chondrocytes at the onset of tissue mineralization and it accumulates in the bone extracellular.

2.2 BLT experiment

The BLT experiment included two steps which is bioluminescent imaging acquirement and the Micro-CT data acquirement.

Mouse was fasted overnight before experiment to avoid the bioluminescence influence of food before experiment. The mouse was fixed at the mouse bed after injecting 200μl urethane, then the mouse bed was assembled in the rotation stage. After intraperitoneal injection of 200μl D-Lucierin (Biotium, Inc. CA, Fremont, USA) four degree images were acquired respectively when the rotation stage was set to rotate by 0^o, 90^o, 180^o and 270^o. Parameters of CCD (Princeton Instruments PIXIS 1024BR, Roper scientific, Trenton, NJ) were set as exposure time =2 min, f-number =2.8, binning =2, controller gain =3, rate = 1 MHz, resolution =16 bits, read out = low noise. As the experiments were carried out in a totally dark environment, we can use a 12-inch integrating sphere (USS-1200V-LL Low-Light Uniform Source, Labsphere Inc., USA) to calibrate the absolute intensity in physical units of the CCD output value. Bioluminescence intensity was counted from the image acquired using Windows Molecular Imaging System (WinMI) software. The four degree bioluminescence images were shown in Fig. 1.

After that, we used Micro-CT system to get the anatomical information. During the imaging acquiring, the parameter of the Micro-CT was set as followings: voltage of X-tuber was 60 kVp, the integration time of detector was 0.467 second, size of each projection view is 1124×1134, pixel size of detector is 0.1mm×0.1mm. On the 90^{th} min after injection of 200μl Fenestra VC through tail vein, 500 projection views were collected in 8.5 minutes. Then we used a GPU accelerated FDK method[10] to reconstruct the volume data. Type of the volume data is 16 bits unsigned short point and the volume size is 512×512×256.

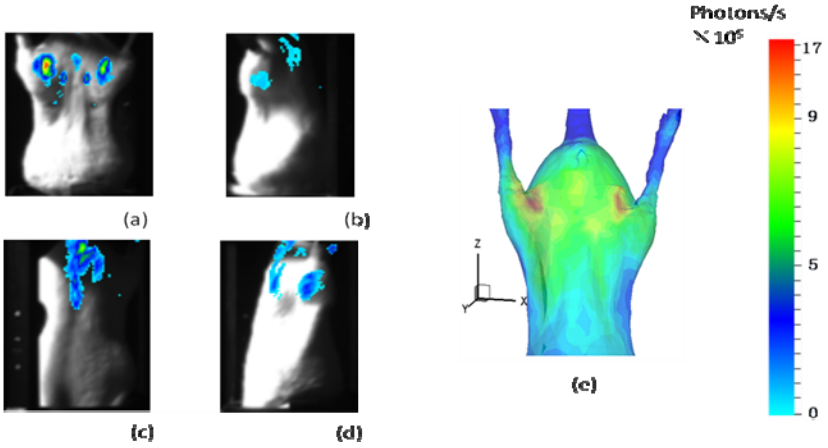

Figure 1: Four overlay images from bioluminescent images and corresponding photographs of the transgenic mouse. (a) Anterior-posterior; (b) left lateral; (c) posterior-anterior; (d) right lateral image.

2.3 Preprocess before reconstruction

After BLT experiments, we need to preprocess the bioluminescent data and the Micro-CT data for the following reconstruction. First, we use MITK to segment and combined the mouse contour and its bone. Then we mapped the bioluminescent intensity to the mouse surface from Micro-CT volume data (shown in Figure 1(e)).

2.4 Reconstruction method

As the imaging experiment was carried out in a totally dark environment, the propagation of bioluminescent photons in the highly scattering biological tissues can be represented by steady-state diffusion equation in bioluminescence tomography[11-12]:

$$-\nabla(D(\mathbf{x})\nabla\Phi(\mathbf{x})) + \mu_a(\mathbf{x})\Phi(\mathbf{x}) = S(\mathbf{x}) \quad (\mathbf{x}\in\Omega) \tag{1}$$

the boundary condition can be depicted as:

$$\Phi(\mathbf{x}) + 2A(\mathbf{x};n,n')D(\mathbf{x})(v(\mathbf{x})\cdot\nabla\Phi(\mathbf{x})) = 0 \quad (\mathbf{x}\in\partial\Omega) \tag{2}$$

Where Ω and $\partial\Omega$ are the domain and its boundary respectively; $\Phi(\mathbf{x})$ denotes the photon flux density [Watts/mm^2]; $S(\mathbf{x})$ is the source energy density [Watts/mm^3]; $\mu_a(\mathbf{x})$ is the absorption coefficient [mm^{-1}]; $D(x) = 1/(3(\mu_a(\mathbf{x}) + (1-g)\mu_s(\mathbf{x})))$ is the optical diffusion coefficient [mm], $\mu_s(\mathbf{x})$ is the scattering coeffient [mm^{-1}], and g is the anisotropy parameter, v is the unit outer normal on $\partial\Omega$. Since the refractive indices n for Ω and n' for the external medium did not match, $A(\mathbf{x};n,n')$ can be approximately represented [11]:

$$A(\mathbf{x};n,n') = \frac{1+R(\mathbf{x})}{1-R(\mathbf{x})} \tag{3}$$

As the mouse is in air, n' is close to 1.0;

$R(\mathbf{x})$ is approximated to $-1.4399n^{-2} + 0.7099n^{-1} + 0.6681 + 0.0636n$ [11]. The measured quantity of the outgoing flux density $Q(x)$ on $\partial\Omega$ is:

$$Q(\mathbf{x}) = -D(\mathbf{x})(v \cdot \nabla \Phi(\mathbf{x})) = \frac{\Phi(\mathbf{x})}{2A(\mathbf{x}; n, n')} \quad (\mathbf{x} \in \partial\Omega) \tag{4}$$

Based on the finite element theory [13], the equation can be finally transformed to

$$AS^p = \Phi^m \tag{5}$$

where Φ^m is the measurable boundary flux, S^p is the unknown source density

So the distributiuon of the bioluminescence source can be calculated through a Tikhonov method with a Newton method handling the optimization procedure.

2.5 *Ex vivo* validation experiment

Beside the *in vivo* experiment, we have done the *ex vivo* experiment to support the reconstruction result. After executing the mice, bones at different locations were cut from the mouse and were digested by enzymatic overnight. The next day, the optical intensity of bone cells in the black 96-plate wells was detected by the BLI system. During the detection, the parameters of the CCD were set as followings: exposure time =30 seconds, f-number =2.8, binning =2, controller gain =3, rate = 1 MHz, resolution =16 bits, read out = low noise. Meanwhile, we had used the chemiluminescence apparatus to detect the intensity of the bone cells. The corresponding results were shown in Figure 3.

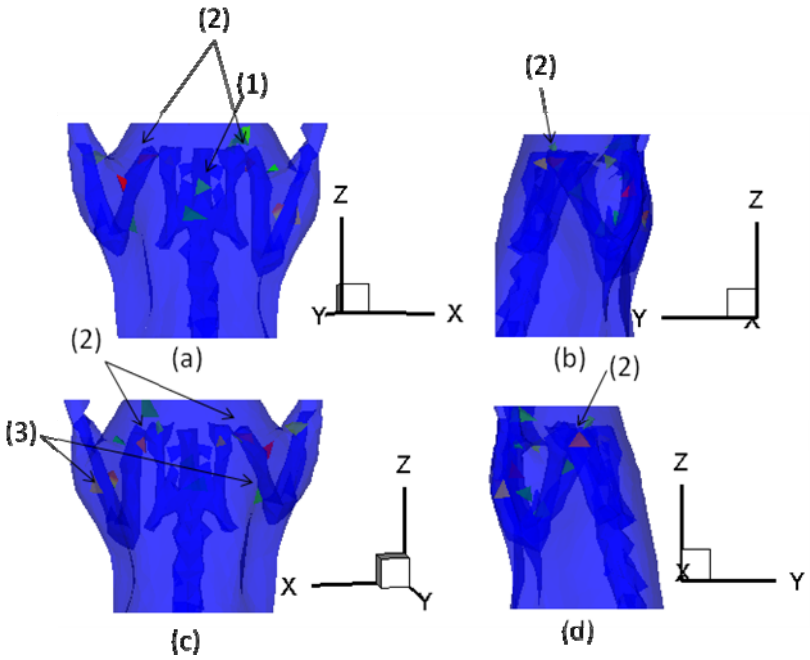

Figure 2: Bioluminescence source reconstructed results. (a) Anterior-posterior; (b) left lateral; (c) posterior-anterior (d) right lateral image. (1) lumbar vertebra; (2) the arthrosis of ischium and femur; (3) femur.

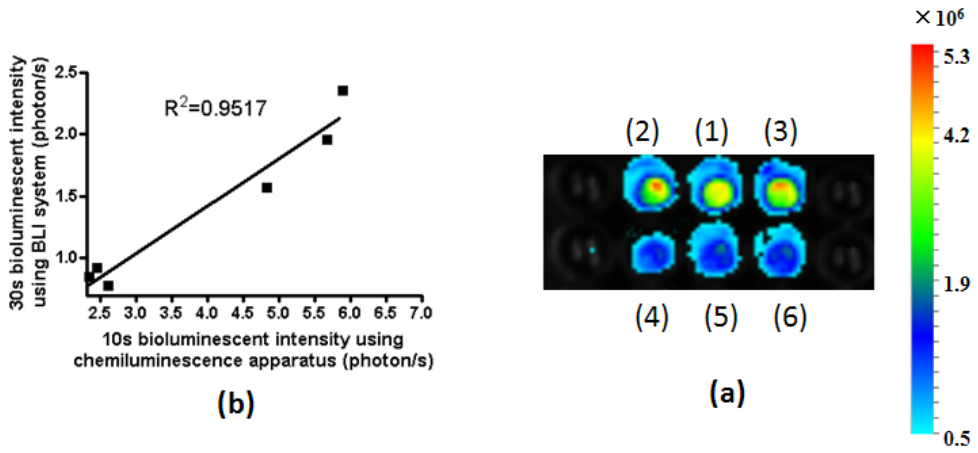

Figure 3: *Ex vivo* results of bone cells at different locations. (a) Bioluminescent imaging using the BLI system, f-number=2.8, exposure time=30s, binning=2; (b) 10 seconds bioluminescence intensity using chemiluminescence apparatus;

Table 1. Correlation of the two bioluminescence intensity results using BLI system and the Chemiluminescence Apparatus (R^2 = 0.9517).

Bone	1	2	3	4	5	6
BLI(10^6 photon/s)	4.83	5.67	5.89	2.60	2.45	2.34
Chemiluminescence Apparatus(10^6 photon/s)	1.57	1.96	2.35	0.78	0.92	0.85

Notes: (1) lumbar vertebra; (2) the arthrosis of ischium and femur; (3) femur; (4) calcaneus; (5) pubis; (6) ischium.

3. RESULTS

According to the reconstructed volume data from Micro-CT, the transgenic mouse was segmented into 2 major organs, including muscle and bone. The reconstruction processor is run according to the parameters of two tissues (as listed in Table 1). The segmented CT volume data was discretized into 3482 points and 19712 tetrahedrons.

Table 2. Optical parameters of different heterogeneous mouse tissues.[14]

Material	μ_a [mm^{-1}]	μ_s [mm^{-1}]	g
Muscle	0.010	4.000	0.900
Bone	0.002	20.000	0.900

In order to induce the ill-posedness of reconstruction, we adopted permissible source region strategy. According to the bioluminescence distribution on the surface after mapping (shown in Fig. 2 (b)), the permissible source region (PS) was set to

$$PS = \{(x, y, z) \mid 12 < x < 38, 10 < y < 30, 60 < z < 71, (x, y, z) \in \Omega\}$$

The regularization parameter was set to 1.0×10^{-12} and the threshold was set to 0.5. The reconstruction time of the aforementioned method was 1269.5 seconds. Based on the heterogeneity of the mouse, the multi-bioluminescence sources in transgenic mOC-Luc mice mouse were reconstructed (shown in Figure 2).

From the reconstruction results, we found that the bioluminescence intensity of arthrosis between

ischium and femur, the femur, the lumbar vertebra were higher than the other sources in the transgenic mOC-Luc mouse. The corresponding quantitative results were shown in table 2. The *ex vivo* results was gained (shown in Figure 3) by calculating the photons of the bone cells. The results show bioluminescence intensity at arthrosis between ischium and femur, the femur, the lumbar vertebra is highest; Bioluminescence intensity at the calcaneus, pubis, ischium is second. The results of the two figures are coherent with each other.

Furthermore, we calculated the reconstructed center of every reconstructed element. The element in the bone nearest to the reconstructed element was considered to be the real elements. Then the error distance (ED) can be calculated through the following equation:

$$ED = \sqrt{(x_1 - x_2)^2 + (y_1 - y_2)^2 + (z_1 - z_2)^2}$$

where (x_1, y_1, z_1) is the real center of the real element, (x_2, y_2, z_2) is the reconstructed center of the reconstructed element.

Table 3. The error distance between reconstructed center of reconstructed element and the real center of real element

Reconstructed Element	Reconstructed Center	Real Element	Real Center	Error distance
(1172, 1215, 1046, 1988)	(15.1, 22.9, 58.8)	(1046, 1215, 1172, 1155)	(15.9, 22.9, 58.6)	0.9
(1447, 1429, 2127, 1527)	(35.8, 18.2, 65.9)	(1310, 1319, 1369, 1342)	(38.5, 16.1, 64.1)	3.9
(1463, 2476, 2521, 2522)	(28.6, 23.2, 66.7)	(1463, 1500, 1530, 1570)	(29.9, 23.1, 68.1)	2.0
(1330, 2419, 3034, 2232)	(22.7, 26.4, 62.0)	(1264, 1330, 1329, 1390)	(24.2, 28.5, 63.1)	2.8
(2531, 3180, 1514, 3179)	(26.8, 24.7, 68.3)	(1532, 1514, 1516, 1552)	(24.2, 24.9, 68.3)	2.6
(3203, 1518, 1537, 3204)	(31.8, 27.0, 68.5)	(1553, 1537, 1518, 1500)	(31.7, 25.6, 68.5)	1.5
(1497, 2525, 1451, 2055	(33.5, 22.4, 68.1)	(1407, 1451, 1550, 1497)	(33.8, 23.5, 67.4)	1.3
(2531, 2529, 1532, 3267)	(26.0, 22.7, 68.2)	(1532, 1514, 1516, 1552)	(24.2, 24.9, 68.3)	2.8
(2201, 2193, 1277, 3416)	(33.8, 21.6, 62.6)	(1277, 1281, 1156, 1234)	(34.3, 23.1, 61.9)	1.6
(1543, 1568, 1582, 1510)	(13.2, 18.9, 67.4)	(1566, 1456, 1446, 1543)	(11.6, 17.4, 67.1)	2.2
(2254, 2169, 2239, 1257)	(13.4, 20.9, 63.4)	(1229, 1290, 1374, 1357)	(11.9, 18.5, 63.4)	2.8
(3463, 2122, 2425, 2346)	(30.9, 20.7, 66.1)	(1463, 1500, 1570, 1462)	(30.6, 23.6, 67.4)	3.2
(1482, 1332, 1466, 1522)	(22.0, 27.9, 66.8)	(1380, 1332, 1482, 3480)	(22.7, 27.6, 66.2)	1.0
(1451, 1550, 1497,	(34.2, 22.9, 68.1)	(1407, 1451, 1550,	(33.8, 23.5, 67.4)	0.9

2055)		1497)		
(1434, 1550, 1451, 3384)	(34.9, 22.6, 67.1)	(1407, 1451, 1434, 1550)	(34.4, 23.4, 66.9)	1.0
(1207, 1225, 2105, 3453)	(35.7, 16.1, 61.4)	(1118, 1207, 1182, 3482)	(36.8, 15.9, 60.6)	1.3

4. CONCLUSIONS

In this paper, the multi-source distribution and intensity in transgenic mOC-Luc mice was reconstructed using multilevel adaptive FEM combined with the temperature control and absolute optical intensity calibration in physical units of the CCD output value. Otherwise, the bioluminescence intensity was monitored by *ex vivo* experiment in black 96-plate wells after executing the mice. The *in vivo* reconstruction result was coincident with the *ex vivo* experiment result. The above results show that multilevel adaptive FEM is effective and accuracy in reconstruction of the inner multi-source distribution. Furthermore, this BLT reconstruction method can facilitate the mechanism study of disease about bone such as osteoporosis, hyperosteogeny etc.

ACKNOWLEDGEMENTS

This paper is supported by the National Basic Research Program of China (973 Program) under Grant 2011CB707700, the Knowledge Innovation Project of the Chinese Academy of Sciences under Grant No. KGCX2-YW-907, the National Natural Science Foundation of China under Grant No. 81027002, 81071205, the Hundred Talents Program of the Chinese Academy of Sciences, the Science and Technology Key Project of Beijing Municipal Education Commission under Grant No. KZ200910005005.

REFERENCES

[1] Zerhouni, E., "Medicine. The NIH Roadmap," Science 302, 63–72 (2003).
[2] Weissleder, R. and Ntziachristos, V., "Shedding light onto live molecular targets," Nat. Med. 9, 123–128 (2003).
[3] Jaffer, F. and Weissleder, R. "Molecular imaging in the clinical area," Jama. pp. 855–862 (2005).
[4] Willmann, J., Bruggen, N., Dinkelborg, L. and Gambhir, S., "Molecular imaging in drug development," Nature **7**, 591-606 (2008).
[5] Weissleder, R., Pittet, M., J., "Imaging in the era of molecular oncology," Nature 452(3), 580-589 (2008).
[6] Ma, X., Liu, Z., Tian, J. and Wang, F., "Dual-Modality Monitoring of Tumor Response to Cyclophosphamide Therapy in Mice with Bioluminescence Imaging and Small-Animal Positron Emission Tomography," Mol Imaging, in press (2010).
[7] Lv, Y., Tian, J., Cong, W., Wang, G., Luo, J., Yang, W. and Li, H., "A multilevel adaptive finite element algorithm for bioluminescence tomography," Opt. Express 14 (18), 8211–8223 (2006).
[8] Wang, G., Shen, H. and Cong, W., "Temperature-modulated bioluminescence tomography," Opt. Express 14, 7852-7871 (2006).
[9] Cong, W. and Durairaj, K., "A born-type approximation method for bioluminescence tomography," Med. Phys. 33, 679-686 (2006).
[10] Yan, G., Tian, J., Zhu, S., Dai, Y. and Qin, C., "Fast cone-beam ct image reconstruction using gpu Hardware," J. X-Ray SCI Technol. 16, 225-234 (2008).
[11] Schweiger, M., Arridge, S., R., Hiraoka, M. and Delpy, D., T., "The finite element method for the propagation of light in scattering media; Boundary and source conditions," Med. Phys. 22, 1779-1792 (1995).

[12] Cong, W., Wang, G., Kumar, D., Liu, Y., Jiang, M., Wang, L., V., Hoffman, E., A., McLennan, G., McCray, P., B., Zabner, J. and Cong, A. "Practical reconstruction method for bioluminescence tomography," Opt. Express 13, 6756-6771 (2005).
[13] Rao, S. S., [The finite element method in engineering], Butterworth-Heinemann, Florida, USA, 50-125 (1999).
[14] Alexandrakis, G., Rannou, F. and Chatziioannou, A., "Tomographic bioluminescence imaging by use of a combined optical-PET (OPET) system: a computer simulation feasibility study," Phys. Med. Biol. 50, 4225-4242 (2005).